Manifold Dynamics and their Applications to Low-Energy Transfers

Presented
by
Jack Tyler

University of Southampton
Southampton, United Kingdom
June 2018

The following work is dedicated to those who did not get to see its' completion.

Brian William Barmby: 1940 - 2008 Diane Patricia Barmby: 1942 - 2010

Contents

List of Figures

List of Tables

Acknowledgments

Firstly, this work would not be possible without the hard efforts of my Supervisor, Dr. Hodei Urrutxua, who decided to take on the first-year who landed in his email inbox one day. I wish to thank Dr. Urrutxua for all the professional and personal development he has afforded me, both in the field of Manifold Dynamics and outside of it.

Similarly, I wish to thank … and Dr. Hugh Lewis for their assistance in seeing me through my years at University, and for allowing me to extend the scope and complexity of this piece.

In a similar vein, I wish to thank Miss India Yardley for the previous three years of happy times – for being there no matter the situation, and making sure I always perform to my best.

And lastly, to Gibson: woof woof, woof. Good boy.

Going to space shouldn't be like pooping pineapples.

Elon Musk

1 The Cost of Access to Space

With advances in launcher technology, the cost of access to space is decreasing rapidly. New innovations in partial-reusability, and the emergence of commercial space – SpaceX, Orbital Sciences, Blue Origin and Virgin Galactic, to name a few – is uprooting the traditional conservatism of the space industry. The 'Billionaire Race', as it is labelled, is providing a driving force for the shakedown of the 'Old Space' community. Aided by the arrival of Moore's Law to the space industry, in the form of nano- and pico-satellites, many space companies are exploiting the use of multiple low-cost satellites to provide the functions of larger, more expensive platforms.

Despite the dramatic reductions in space cost, it is rare that payloads are injected into their final orbit by their launch vehicle. Mission designers are posed with an optimisation problem for every trajectory and mission plan they undertake; that is, the arrival and maintaining of the spacecraft at its' nominal orbit for the least amount of propellant mass. In the case of space missions, which often end when their available propellant is expended, the minimisation of propellant usage is of utmost importance.

The language of mission designers is not without the perpetual usage of the term ΔV: the overall velocity – and thus propellant – required to undertake a maneouvre.

Konstantin Tsiolkovsky first determined the relationship between velocity increments and propellant mass in 1903, which became one of the most famous and widely-used equations in rocket science, relating the velocity increment ΔV to the exhaust velocity v_e and the ratio of initial to final masses (Curtis, 2010):

$$\Delta v = v_e \ln\left(\frac{m_0}{m_f}\right) \tag{1.1}$$

Equation 1.1 is the most important equation of all in mission design. Its' tyranny – a term coined for its' logarithmic nature in increasing Δv – places large limits on attainable destinations in the solar system, and gravity assists from planetary bodies are often required to reach the corners of the solar system with any useful payload mass remaining.

The optimisation problem brought on by Equation 1.1 has led to the advent of many techniques for the reduction of propellant mass in space mission design. Perhaps one of those given most attention is the prospect of the *low-energy transfer*. A *low-energy transfer* utilises far less propellant than

[*] Yet to fly.

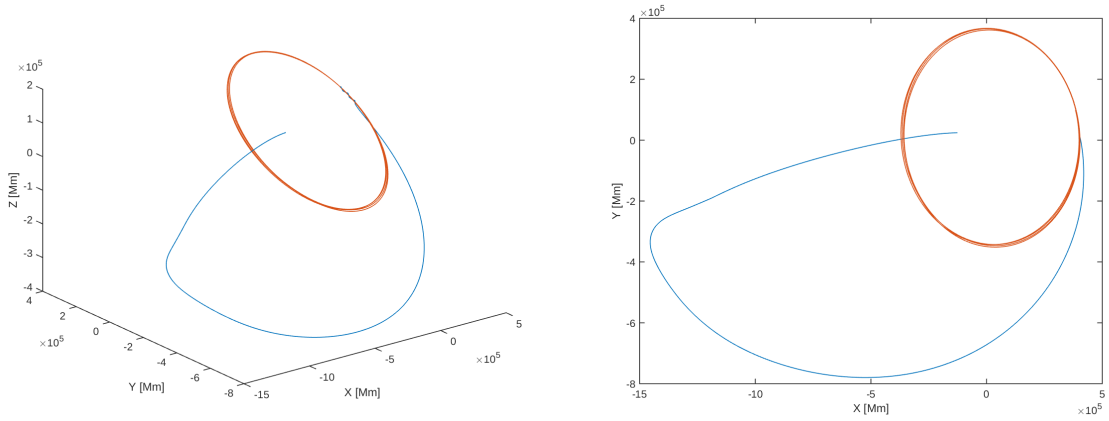

Figure 1.1: The transfer trajectory of NASA's GRAIL spacecraft in the ICRF/J2000 frame. Ephemeris supplied by JPL.

a more traditional transfer, such as a Hohmann or bi-elliptic transfer, but often at the cost of transit times. Further, the computation of these transfers and trajectories can be delicate, and often exist as a complex harmony of gravitation and chaos.

The first mission to undertake such a transfer was *Hiten*, a Japanese probe launched to the vicinity of the Moon in 1990. Originally named MUSES-A, its' daughter payload experienced a failure upon injection into Lunar orbit. (Belbruno and Miller, 1993) devised a new method of transfer – the *weak stability transfer* – that would allow for injection of MUSES-A, now renamed *Hiten*, into Lunar orbit itself. While a lengthy transit time of five months was present, the capture into Lunar orbit required zero Δv, and allowed for the transfer to be conducted by the probe's on-board thrusters.

Further exploitation of these types of transfers followed, with NASA's GRAIL satellite utilising an exterior weak-stability transfer to transit to the Moon (Figure 1.1. The European Space Agency's SMART-1 mission employed an interior weak-stability transfers to transit to the Moon using low-thrust.

These *low-energy transfers* are the offspring of the applications of dynamical systems theory to space mission design. A particular case of orbital motion, the three-body problem, yields many dynamical structures - stable and unstable manifolds and bounding surfaces - that provide phase-space structures for the transfer of objects into and from the smaller primary body. The use of these dynamical phenomena can provide advantages to the mission designer for dramatic propellant savings.

The following work acts as an introduction to the application of dynamical systems theory to space mission design. Section 2 provides a brief introduction to the three-body problem, and includes a derivation from the Newtonian n-body problem. A small understanding of orbit theory is assumed, and the Section goes on to cover the zero-velocity curves and forbidden regions of the three-body problem, and its' pseudo-potential and integral of motion, the Jacobi constant. Section **??** lays out an introduction to the numerical methods and techniques used to design and construct orbits in the three-body problem, including Poíncaré maps, single- and multiple-shooting, and numerical integration. From this, we construct an example halo orbit, and use it to introduce the concept of Stable Manifolds. These phenomena are further analysed and formally introduced in Section 4. The exploitation of these phenomena follows in Section **??**.

Throw two planets into space, and they will fall one on the other...it is a fatality, a question of time; that is all.

Jules Verne

2

An Introduction to the Three-body Problem

The three-body problem has admitted a 'star-studded line-up' of mathematicians to its' study; names such as (Euler, 1736), (Jacobi, 1829) and (Poincaré, 1899) performed a lot of the early work on its' formulation.

Its' inception is believed to have begun with (Euler, 1736) [WRONG - 1767], who introduced a synodic coordinate system during his studies of Lunar motion. In fact, this co-ordinate system admitted a constant of motion, later to be 'discovered' by (Jacobi, 1829) to be the well-known Jacobi integral. Euler's work also contained a solution of the motion of a third body under the action of two fixed force centers. Whilst this postulation neglects the centrifugal and Coriolis forces, it yields a solution and thus provides numerous applications. In particular, this solution is sometimes applied as a reference orbit for general-perturbation theory (Szebehely, 1967).

One of the next significant contributions came with (Jacobi, 1829), who re-discovered – to the tongue-in-cheek remark of Wintner – the integral of motion in the three-body problem and his namesake. The Jacobian is an important integral in the three-body problem, for it relates the magnitude of the velocity vector to the location of the third mass. In a system with no solution expressible by algebraic relations, the Jacobi integral can qualitatively imply characteristics of the third body's motion without the solution to the governing equation.

(Hill, 1906) later used the Jacobi integral to prove that the Earth-Moon distance is bounded from above; the integral predicts a 'forbidden region', for which the motion of the third mass cannot enter.

Euler [1772, reference] studied the motion of the Moon assuming the paths of the Earth and the Sun are circular, and that the mass of the Moon was negligible; a study now known as the *restricted three-body problem*. Lagrange [1772, reference] discovered the equilateral triangle solutions; together with the collinear solutions, these solutions are the only explicit solutions for arbitrary masses.

The classical period of study for the three-body problem ended when the methods of section, phase-space and deterministic chaos were developed by Poincaré. For this, Sweden's King Oscar II awarded Poincaré a prize to award him for being the first to solve the n-body problem (although he did not, in fact, even solve the general case of the three-body problem.)

The following section derives the governing equations of motion for the Newtonian n-body problem, as a key piece of background introductory material for the formulation of the three-body problem, a particular case for $n = 3$.

We wish to study the motion of a kth particle under the influence of $n \geqslant 2$ bodies, which moves in three-dimensional space x_1, x_2, x_3 under the influence of Newtonian inverse-square gravitation. We state that the Cartesian coordinates of such a particle are given by $(x_{k1}, x_{k2}, x_{k3}) \in \mathbb{R}^3$ and thus that the differential equations that define the motion of such a particle are given by:

$$m_k \ddot{x}_k = \sum_{\substack{j=1 \\ j \neq k}}^{n} \frac{G m_j m_k}{\boldsymbol{r}^2_{jk}} \frac{\boldsymbol{x}_j - \boldsymbol{x}_k}{r_{jk}} \tag{2.1}$$

for $k = 1, 2, ..., n$ and where $r_{jk} = |\boldsymbol{x}_j - \boldsymbol{x}_k| = \sqrt{\sum_{i=1}^{3} (x_{ji} - x_{ki})}$ is the Euclidean distance between the kth and ith particles. Equation 2.1 states that the kth particle P_k moves under the sum of the forces from the $n-1$ particles P_n, $n = 1, 2, 3..., n-1$, and represents $3n$ second-order differential equations.

If we linearise Equation 2.1 and divide by m_k:

$$\begin{aligned} \dot{\boldsymbol{x}}_k &= \boldsymbol{v}_k \\ \boldsymbol{v}_k &= m_k^{-1} \frac{\partial U}{\partial \boldsymbol{x}_k} \end{aligned} \tag{2.2}$$

then we obtain the velocity of the kth particle $\boldsymbol{v}_k = (v_{k1}, v_{k2}, v_{k3}) = (\dot{x}_{k1}, \dot{x}_{k2}, \dot{x}_{k3}) \in \mathbb{R}^3$, where U is the potential energy and G the universal gravitational constant.

$$U = \sum_{\substack{j=1 \\ j \neq k}}^{n} \frac{G m_j}{r_{jk}} \tag{2.3}$$

$\frac{\partial U}{\partial \boldsymbol{x}_k}$ is a real function of three variables that yields $6n$ first order differential equations; further, if $r_{jk} > 0$, then U is smooth – it has partial derivatives for all orders of variables and is real analytic. Inspection of Equation 2.3 reveals that it is of the form $\dot{\boldsymbol{y}} = \mathrm{f}(\boldsymbol{y}); \boldsymbol{y} = (\boldsymbol{x}, \boldsymbol{v}) \in \mathbb{R}^{6n}$, and we can thus apply standard uniqueness and existence theorems (and by implication, also to Equation 2.2). This $(6n+1)$ dimensional relationship – $\boldsymbol{x_{kj}}, \boldsymbol{v_{kj}}, t$ – can be reduced by finding an integral solution to Equation 2.1 , which is a real-valued function of the $(6n+1)$ variables, and is constant through a solution to 2.1. If we denote a solution as $\boldsymbol{x}(t), \boldsymbol{v}(t)$, then we arrive at the conclusion that the integral of 2.1, $I(\boldsymbol{x}, \boldsymbol{v}, t)$, is such that:

$$\frac{d}{dt} I(\boldsymbol{x}(t), \boldsymbol{v}(t), t) = 0 \tag{2.4}$$

which implies that the integral is constant through the given solution, defining a $6n$-dimensional integral manifold on which the solutions lie.

$$I^{-1}(0) = \{(\boldsymbol{x}, \boldsymbol{v}, t) \in \mathbb{R}^{6n+1} | I = c\} \tag{2.5}$$

This integral constrains the motion of the particle by solving for one variable as a function of the other six. We define the $6n$-dimensional state of coordinates to be the phase space: $(\boldsymbol{x}, \boldsymbol{v}) \in \mathbb{R}^{3n} \times \mathbb{R}^{3n}$ and the extended phase space to be inclusive of the extra dimension t: $(\boldsymbol{x}, \boldsymbol{v}, t) = \mathbb{R}^3 \times \mathbb{R}^3 \times \mathbb{R}^1$.

Equation 2.1 yields 10 independent algebraic integrals, provided by the conservation of momentum – both linear and angular – and energy. To begin, we may add 2.1 to derive linear momentum conservation:

$$\text{LHS:} \sum_{k=1}^{n} m_k \ddot{\boldsymbol{x}}_k \tag{2.6}$$

$$\text{RHS:} \sum_{k=1}^{n} \sum_{j=1}^{n} \frac{G m_j m_k}{r_{jk}^2} \frac{\boldsymbol{x}_j - \boldsymbol{x}_k}{r_{jk}} \tag{2.7}$$

The RHS is 0, due to cancellations of negatives from the summation, and thus we may imply:

$$\sum_{k=1}^{n} m_k \ddot{\boldsymbol{x}}_k = 0 \tag{2.8}$$

If we take the vector centre of mass for the particles to be $\boldsymbol{\rho} = (\rho_1, \rho_2, \rho_3) \in \mathbb{R}^3$, and thus $\ddot{\boldsymbol{\rho}} = 0$:

$$M = \sum_{k=1}^{n} m_k, \;\; \rho = M^{-1} \sum_{k=1}^{n} m_k \boldsymbol{x}_k \tag{2.9}$$

Yielding:

$$\boldsymbol{\rho} = \boldsymbol{c_1} t + \boldsymbol{c_2} \tag{2.10}$$

where $\boldsymbol{c_1}, \boldsymbol{c_2}$ provide six constants to be unique from the initial conditions at $t = t_0$ [*].

For analysis, we may move the origin of the Cartesian coordinate system x_1, x_2, x_3 for motion of the kth particle through a shift:

$$\bar{x}_j = x_j - \rho_j \tag{2.11}$$

without alteration of Equation 2.1, since $\ddot{\rho}_j = 0$. An assumption can therefore be made that $\boldsymbol{\rho} = 0$, and as such:

$$\sum_{k=1}^{n} m_k \boldsymbol{x}_k = 0, \;\; \sum_{k=1}^{n} m_k \boldsymbol{v}_k \tag{2.12}$$

which represent six independent algebraic integrals. Considering the conservation of energy:

$$\xi = \text{KE} - \text{U} \tag{2.13}$$

where U is the potential energy, as before, and KE the kinetic energy of the system:

$$\text{KE} = \frac{1}{2} \sum_{k=1}^{n} m_k |\boldsymbol{v}_k|^2 \tag{2.14}$$

and is thus our 7^{th} integral, since Equation 2.3 implies that the time derivative of $T - U = 0$ [†].

[*] Note that Equation 2.10 gives the law of the conservation of linear momentum – that the center of mass moves uniformly in a straight line.

[†] Energy is constant along solutions.

The 8^{th}, 9^{th} and 10^{th} integrals are provided by the conservation of angular momentum, using the vector cross product of Equation 2.1 $\boldsymbol{x}_k \times \ddot{\boldsymbol{x}}_k$:

$$\sum_{k=1}^{n} m_k(\boldsymbol{x}_k \times \ddot{\boldsymbol{x}}_k = \sum_{k=1}^{n}\sum_{j=1}^{n} \frac{Gm_j m_k}{r_{jk}^3}\boldsymbol{x}_k \times \boldsymbol{x}_j = 0 \tag{2.15}$$

$j \neq k$ since $\boldsymbol{x}_k \times \boldsymbol{x}_k = 0$ and $\boldsymbol{x}_k \times \boldsymbol{x}_j = -\boldsymbol{x}_j \times \boldsymbol{x}_k$. Integrating the LHS of 2.10 reports:

$$\sum_{k=1}^{n} \boldsymbol{x}_k \times \boldsymbol{v}_k = \boldsymbol{c} \tag{2.16}$$

$\boldsymbol{c} = (c_1, c_2, c_3) \in \mathbb{R}^3$‡.

The Circular-Restricted Three-Body Problem

The establishment of some sort of geometric model is necessary for the computation of the secondary mass m_3. We define an intertially-fixed coordiate system with its' origin at the barycenter of the primary masses (Mains, 1993) in the $\bar{x}$, $\bar{y}$, $\bar{z}$ axes. The $\bar{x}$ and $\bar{y}$ axes are in the plane of the two primaries, with $\bar{z}$ completing the right-handed coordinate system.

Another system, the rotating coordiante system, is also located at the barycenter of the system, with its' $\bar{X}$ axis directed from the larger primary to the smaller primary. The $\bar{Z}$ axis is coincident with its' partner $\bar{z}$ axis, with $\bar{Y}$ completing the coordinate system. We define θ as the angle between the respective $\bar{x}$ and $\bar{X}$ coordinate systems. The angular velocity of the system is constant.

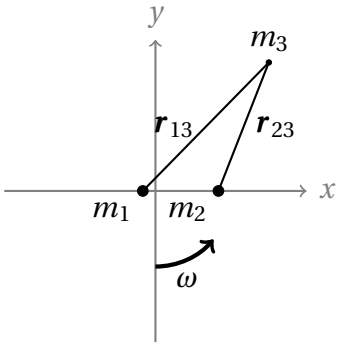

Figure 2.1: Rotating co-ordinate system used in the formulation of the governing equations of motion in the three-body problem.

We wish now to use this general form for n-body motion to determine the motion of a mass m_3 under the influence of two far larger masses m_1 and m_2, $m_1 > m_2$. Returning to Equation 2.1 and setting the number of particles $n = 3$:

$$\sum F = \frac{Gm_3 m_2}{r_{23}^3}\boldsymbol{r_{23}} - \frac{Gm_3 m_1}{r_{13}^3}\boldsymbol{r_{13}} = m_3\ddot{\boldsymbol{r}}_3 \tag{2.17}$$

we may use a number of assumptions to simplify our analysis. Namely:

- We assume that, for generality, $m_1 > m_2 >> m_3$;
- Orbits are circular and occur about the pmbycenter of the system;

‡For more information regarding the implication of the value of this constant on the state of the system, refer to (Belbruno, 2004)

Mass parameter	$\mu = \frac{m_2}{M}$
Mass of m_2	μ
Mass of m_1	$1-\mu$
Coordinates of the center of mass of m_1	$\rho_1 = (-\mu, 0)$
Coordinates of the center of mass of m_2	$\rho_2 = (1-\mu, 0)$
Gravitational constant G	1
Angular velocity of the system	1
Period of the two larger masses	2π

Table 2.1: Normalisations used in the CR3BP

- Only gravitational forces act on the masses;
- The masses are of a sufficient size and characteristic to regard them as point masses.

Further, we normalise the system using the mass parameter μ, defined as in Equation 2.18:

$$\mu = \frac{m_2}{M},\ M = m_1 + m_2 \tag{2.18}$$

which implies the normalisations outlined in Table **??**. If we non-dimensionalise Equation 2.17, we obtain Equation 2.19.

$$\ddot{\boldsymbol{r}}^{i}_{m_3} = -\frac{1-\mu}{r_{13}^3}\boldsymbol{r}_{13} - \frac{\mu}{r_{23}^3}\boldsymbol{r}_{23} \tag{2.19}$$

Considering the inertial frame of reference, we express the velocity of m_3 using the rotating frame and the angular velocity:

$$\dot{\boldsymbol{r}}^{I}_{m_3} = \boldsymbol{r}^{R}_{m_3} + \omega_{I\times R} \times \boldsymbol{r}_{m_3} \tag{2.20}$$

recalling that $\omega_{I\times R}$ is unity, and thus $\omega_{I\times R} = \hat{\gamma} = \hat{z}$ we may write in the inertial frame:

$$\dot{\boldsymbol{r}}_{m_3} = (\dot{x} - y)\hat{x} + (x + \dot{y})\hat{y} + \omega_{I\times R} \times \boldsymbol{r}_{m_3} = (\dot{x} - y)\hat{x} + (x + \dot{y})\hat{y} + \dot{z}\hat{z} \tag{2.21}$$

and the derivative with respect to time yields Equation 2.22.

$$\ddot{\boldsymbol{r}}^{i}_{m_3} = (\ddot{x} - 2\dot{y} - x)\hat{x} + (\ddot{y} + 2\dot{x} - y)\hat{y} + \ddot{z}\hat{z} \tag{2.22}$$

Equating Equations 2.19 and 2.22 gives the following:

$$(\ddot{x} - 2\dot{y} - x)\hat{x} + (\ddot{y} + 2\dot{x} - y)\hat{y} + \ddot{z}\hat{z} = -\frac{1-\mu}{r_{13}^3}\boldsymbol{r}_{13} - \frac{\mu}{r_{23}^3}\boldsymbol{r}_{23} \tag{2.23}$$

and we thus arrive at the system of equations that governs the motion of the mass m_3, with r_{13}^2 and r_{23}^2 the Eucliean distances between the primary and secondary to the third body, respectively:

$$r_{13}^2 = (x+\mu)^2 + y^2 + z^2 \tag{2.24}$$

$$r_{23}^2 = (x-1+\mu)^2 + y^2 + z^2 \tag{2.25}$$

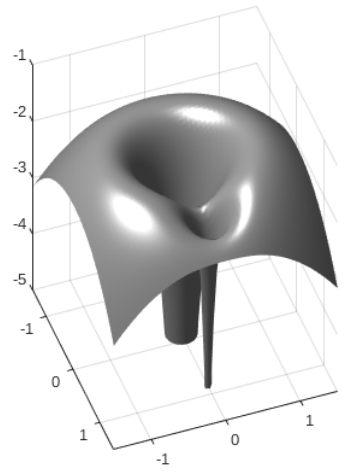

Figure 2.2: The pseudo-potential in the Earth-Moon system for $\mu = 6$

As mentioned previously, the three-body problem admits an integral of motion, the Jacobi constant. To determine this, we first seek to formulate a pseudo-potential, Ω, through integrations of the right-hand side of Equation 2.23, with respect to the variables x, y and z, respectively:

$$\Omega_x = \frac{x^2}{2} + \frac{1-\mu}{r_1 3} + \frac{\mu}{r_{23}} + f(y,z) \tag{2.26}$$

$$\Omega_y = \frac{y^2}{2} + \frac{1-\mu}{r_{13}} + \frac{\mu}{r_{23}} + f(x,z) \tag{2.27}$$

$$\Omega_z = \frac{1-\mu}{r_1} + \frac{\mu}{r_{23}} + f(x,y) \tag{2.28}$$

Which we may write as a function of particle position and the mass parameter only.

$$\Omega = \frac{1}{2}(x^2 + y^2) + \frac{1-\mu}{r_{12}} + \frac{\mu}{r_{23}} \tag{2.29}$$

As a result, with slight rearranging, we may report the governing equations of motion in Equation 2.23 as functions of the pseudo-potential.

$$\ddot{x} - 2\dot{y} = \frac{\partial \Omega}{\partial x} \tag{2.30}$$

$$\ddot{y} + 2\dot{x} = \frac{\partial \Omega}{\partial y} \tag{2.31}$$

$$\ddot{z} = \frac{\partial \Omega}{\partial z} \tag{2.32}$$

Figure 2.2 reports a plot of the pseudo-potential in the Earth-Moon system; the measurement of the position and velocity of the mass m_3 determines the energy associated with its' motion.

The Jacobi Constant

The Jacobi integral admits the constant of motion for the three-body problem. We may derive the Jacobi integral from the equations of motion in 2.23:

$$\frac{\mathrm{d}}{\mathrm{d}t}(\dot{x}^2 + \dot{y}^2 + \dot{z}^2) = 2(\dot{x}\ddot{x} + \dot{y}\ddot{y} + \dot{z}\ddot{z}) \tag{2.33}$$

which, when including expressions for $\ddot{x}$ and the other position variables from Equation 2.30, reads:

$$\frac{\mathrm{d}}{\mathrm{d}t}(\dot{x}^2 + \dot{y}^2 + \dot{z}^2) \tag{2.34}$$

$$= 2[\dot{x}(2\dot{y} - \Omega_x) + \dot{y}(-2\dot{x} - \Omega_y) + \dot{z}(-\Omega_z)] = 2\frac{\mathrm{d}}{\mathrm{d}t}(-\Omega) \tag{2.35}$$

and thus, we obtain the Jacobi constant:

$$C = -(V^2 + \Omega),\ V = (\dot{x}^2 + \dot{y}^2 + \dot{z}^2) \tag{2.36}$$

which represents the energy state of the mass m_3.

Forbidden Regions

With the determination of the value of the Jacobi constant in Equation 2.36, we may inspect the concept of forbidden regions, or Hill's curves, from the namesake (Hill, 1906). Noting that the energy state is dependent on the velocity and position of the particle only, a given value of the energy integral will permit motions in only certain regions of the three-body system. For example, consider the cases outlined in Figure 2.3:

- $C = 5.00$: here, the energy of the mass m_3 is relatively small (for example, consider a spacecraft after injection into LEO), and the regions of travel for the spacecraft are similarly limited. The spacecraft possesses the energy necessary to move along any path that is perturbation free within the vicinity of the larger mass m_1 – this is often named the 'interior realm'
- Suppose the spacecraft makes a maneouvre to increase its' velocity – and thus energy – to a value $C = 4.2$. This opens up a new region of space available for exploration along a perturbation-free path with the 'necking' of the Earth-Moon line.
- For increasing values of C, for example $C = 3.92$, more regions of space becomes available for the mass to access, leading to the access to the 'exterior realm'. Eventually, as is with the case $C = 3.2$, the entire Earth-Moon system is available for traversal (although such a scenario is unfavourable for many locations: we seek to arrive at a point with the least amount of energy expended.)

The motion for which we are most interested in is for case 3, when the spacecraft may traverse either the exterior or interior regions through means of motion through the 'neck' point around the second primary. We will discover in Section **??** that the motion in this region is controlled by the invariant manifold structures in the region.

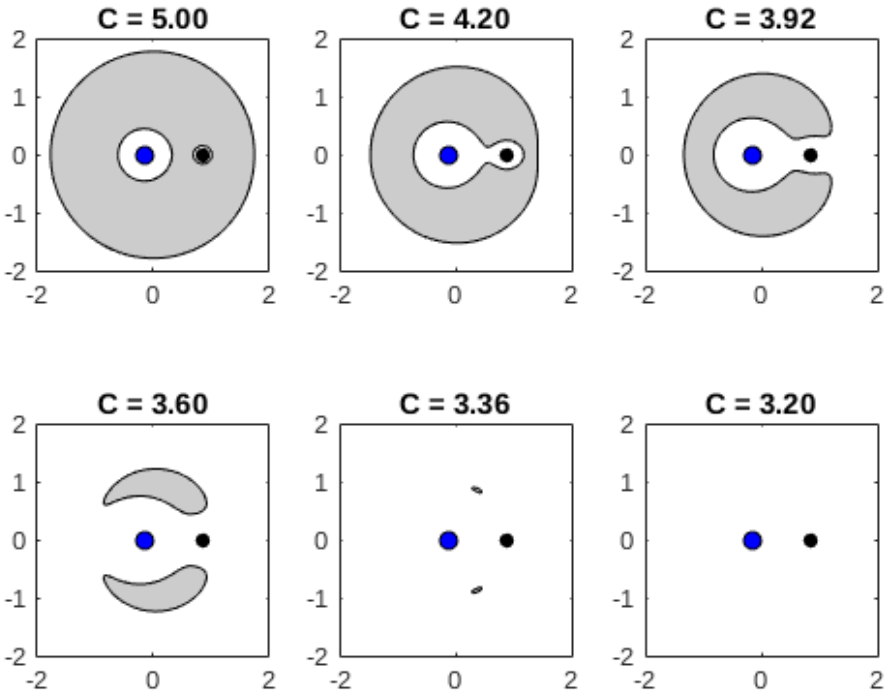

Figure 2.3: Forbidden regions in the Earth-Moon system for different values of the Jacobi constant; the forbidden regions are shaded in grey; the value of $C = 3.92$, where the inner and outer regions have just become available to the particle, are of the most interest.

We focus particularly on case 3, where the movement between the exterior and interior realm is controlled by motion through the 'neck' region. In this section, we examine the motion of a particle around the lagrangian points as a precursor for trajectories in the neck region, and examine linearisations and characteristics of the motion around these points.

We begin by considering the Lagriangian case of motion expressed in Equation 2.30, and translating the origin of the frame to one of the collinear points L_i. Denoting ϕ to be the distance from L_i to the smaller primary (positive when referring to L_2 and negative with respect to L_1 and L_3), we obtain the new positional coordinates x', y' and z':

$$x' = x - (1 - \mu + \phi) \tag{2.37}$$
$$y' = y \tag{2.38}$$
$$z' = z \tag{2.39}$$

and for which the linearisation of Equation 2.23 under this transformation yields:

$$\ddot{x}' - 2\dot{y}' - (1 + 2\alpha)x' = 0 \tag{2.40}$$
$$\ddot{y}' + 2\dot{x}' + (\alpha - 1)y' = 0 \tag{2.41}$$
$$\ddot{z}' + \alpha z' = 0 \tag{2.42}$$

where α is a constant coefficient. Whilst the solution for the z-plane motion is simple harmonic, the in-plane $x - y$ motion involves a characteristic equation in real and imaginary domains; each root represents a mode of motion, one divergent and one non-divergent ADD IN LOW-ENERGY LUNAR REFERENCE HERE. Exciting the non-divergent mode of motion represents a bounded solution.

$$x' = -kA_y \cos(\lambda t + \psi) \tag{2.43}$$
$$y' = A_y \sin(\lambda t + \psi) \tag{2.44}$$
$$z' = A_z \sin(\sigma t + \beta) \tag{2.45}$$

Equations 2.43 through 2.45 represent six variables in the mode of motion; A_y and A_z represent the amplitudes of in-plane and out-of-plane motion, respectively; λ and σ the frequency of oscillations in the in- and out-of-planes, and the phase angles for the two planes, ψ and β. Indeed, it simple to conclude that the solutions to motion around the Lagrange points are characterised by oscillatory motion. With respect to the two frequencies λ and σ, two distinct cases of orbit types emerge:

- If the two frequencies are commensurate [§], the resulting motion is periodic; further, if these are equal, the particle will enter into a halo orbit.
- If the two frequencies are incommensurate, the motion is quasiperiodic, commonly known as Lissajous orbits.

[§]From (Heath and Euclid, 1956): two linked variables are commensurate if their ratio is a rational number.

Further, setting A_z to zero and thus constraining the motion into the $x-y$ plane will yield Lyapunov orbits. Lyapunov orbits have dynamics well represented by the relatively simple linearised dynamics provided above, and may thus be formulated analytically.

Figure **??** provides an example of sets of Lyapunov orbits; note that the three-body problem exhibits symmetry about $y = 0$. As a result, there are two families of each type of orbit: 'northern' and 'southern' orbits. Particles are categorised into each depending on the dominant amount of time spent in each region.

We will see in Section **??** a more advanced method of constructing Halo orbits using forward shooting and differential correction.

3

Numerical Computation of Motion about the Lagrange Points

The construction of low-energy transfers requires the implementation of numerical techniques and methods. The following section introduces and discusses key methods and tools to analyse and construct low-energy transfers in the three-body problem. These methods are then demonstrated in the construction of a Halo orbit using single forward shooting techniques.

PERHAPS AN INTRODUCTION TO THE NUMERICAL COMPUTATION WORK SO FAR???

Poincayrei maps

The State Transition Matrix

The state transition matrix is a key tool for monitoring divergent dynamics through a trajectory. For the purposes of the construction of orbital transfers, it has the following uses:

- providing a means of adjusting initial conditions of a trajectory to correct for variations in desired final conditions;
- providing a means of examination of orbit stability, and eigenvector orientations (Parker and Anderson, 2014).

To this end, the state transition matrix is essential for differential correction techniques (Section 3.3). As in (Howell et al., 1997), if we suppose that we have some state vector at a time t, $\bar{\boldsymbol{x}} = [x, y, z, \dot{x}, \dot{y}, \dot{z}]^T$, we may obtain an approximation relative to some reference solution using a Taylor series expansion. Ignoring higher order terms, this computes as:

$$\delta \dot{\boldsymbol{x}} = A(t)\, \delta \bar{\boldsymbol{x}}(t) \tag{3.1}$$

where $A(t)$ is a 6x6 time varying matrix of 3x3 sub-matrices:

$$A(t) = \begin{bmatrix} 0 & I_3 \\ U & 2\,\Omega \end{bmatrix} \tag{3.2}$$

with

$$\Omega = \begin{bmatrix} 0 & 1 & 0 \\ -1 & 0 & 0 \\ 0 & 0 & 0 \end{bmatrix} \tag{3.3}$$

and

$$U = \begin{bmatrix} U_{xx} & U_{xy} & U_{xz} \\ U_{yx} & U_{yy} & U_{yz} \\ U_{zx} & U_{zy} & U_{zz} \end{bmatrix} \tag{3.4}$$

where U_{ab} represents $\frac{\partial U}{\partial a\, \partial b}$, and U is symmetric if all derivatives of all orders are continuous. Referring back to Equation 3.1, we note the solution of Equation 3.1 is of the form:

$$\delta \dot{\boldsymbol{x}}(t) = \Phi(t, t_0)\, \delta \boldsymbol{x}(t_0) \tag{3.5}$$

where $\Phi(t, t_0)$ implies the state transition matrix propagated from time t_0 to time t. The elements of Φ correspond to the matrix partial, which represents the sensitivity in the state at time t following a small perturbation at time t_0.

$$\Phi(t) = \frac{\partial \boldsymbol{x}(t)}{\partial \boldsymbol{x}(t_0)} \tag{3.6}$$

Differentiation of Equation 3.6 and substitution of Equations 3.1 and 3.6 yields:

$$\delta \dot{\boldsymbol{x}} = A(t)\, \delta \boldsymbol{x}(t) = \dot{\Phi}(t, t_0)\, \delta \boldsymbol{x}(t_0) + \Phi(t, t_0)\, \delta \dot{\boldsymbol{x}}(t_0) = A(t)\, \delta \boldsymbol{x}(t) = \dot{\Phi}(t, t_0)\, \delta \boldsymbol{x}(t_0) \tag{3.7}$$

and thus

$$\dot{\Phi}(t, t_0) = A(t)\, \Phi(t, t_0) \tag{3.8}$$

which represents 36 first order differential equations for iteration through the orbit propagation[*]. The initial conditions for Equation 3.8 are provided by a 6×6 identity matrix.

The Monodromy Matrix and Floquet's Theorem

A special case of the state transition matrix, the monodromy matrix provides a determination of the stability of a periodic orbit (Russell, 2006); for an unstable orbit, the monodromy matrix yields at least one eigenvalue outside the unit circle. In the CR3BP, the monodromy matrix typically contains 6 eigenvalues occurring in reciprocal pairs (Broucke, 1968), λ_i, $i = 1, 2, ..., 6$, corresponding to six eigenvectors $\boldsymbol{v}_i$. These eigenvalues are roots of a characteristic equation, with a characteristic exponent $e^{\alpha T}$, where T is the period of the orbit[†]. The computation of the eigenvalue reveals the stability of the periodic orbit under a perturbation; referring to Table **??**:

- We say an orbit is stable if the eigenvalues are in the range (-1, 1);
- an orbit is neutrally stable if the eigenvalue is equal to -1 or 1;
- an orbit is unstable if the eigenvalue is outside the range [-1, 1];

[*] These equations are also known as the variational equations

[†] This exponent is sometimes referred to as the Lyapunov characteristic exponent.

(Broucke, 1968) states that it is customary to ignore the invariant presence of unity eigenvalues when assessing stability. Broucke also provides a computationally fast method for the determination of eigenvalues λ_1 through λ_6:

Eigenvalue	**Result of Perturbation**
Real, $< 1, > -1$	Exponential decay
Real, $= 1$ or $= -1$	Neither decay nor growth
Real, $\geq 1, \leq 1$	Exponential growth
Imaginary	The perturbation oscillates about the spacecraft's original state

Table 3.1: Effects of Lyapunov characteristic exponent on perturbation state for a periodic orbit

$$\det(M-\lambda I) = (\lambda-\lambda_1)(\lambda-\lambda_2)(\lambda-\lambda_3)(\lambda-\lambda_4)(\lambda-\lambda_5)(\lambda-\lambda_6) = 0 = (\lambda-1)^2(\lambda-\lambda_1)(\lambda-1/\lambda_1)(\lambda-\lambda_3)(\lambda-1/\lambda_3) \tag{3.9}$$

which, if written in terms of intermediate variables p and q:

$$(\lambda-1)^2 = 0;\ \lambda^2 + p\lambda + 1 = 0;\ \lambda^2 + q\lambda + 1 = 0 \tag{3.10}$$

with $p = -(\lambda_1 + 1/\lambda_1)$, $q = (-\lambda_3 + 1/\lambda_3)$. Factoring 3.10 yields:

$$(\lambda-1)^2\lambda^4 + (p+q)\lambda^3 + (pq+2)\lambda^2 + (p+q)\lambda + 1 = 0 \tag{3.11}$$

and with the introduction of another set of new parameters β, γ and δ, we observe:

$$(\lambda-1)^2\lambda^4 + \beta\lambda^3 + \gamma\lambda^2 + \beta\lambda + \delta = 0 \tag{3.12}$$

which implies $\beta = p + q$, $\gamma = pq + 2$ and $\delta = 1$. Working backwards from these parameters can yield values of the eigenvalues:

$$\beta = 2 - \text{trace}(M) \tag{3.13}$$

$$\gamma = \frac{\beta^2 - \text{trace}(M^2)}{2} + 1 \tag{3.14}$$

then

$$p,\ q = \frac{\beta \pm \sqrt{\beta^2 - 4\gamma + 8}}{2} \tag{3.15}$$

and

$$\lambda_1,\ 1/\lambda_1 = \frac{-p \pm \sqrt{p^2-4}}{2} \tag{3.16}$$

$$\lambda_3,\ 1/\lambda_3 = \frac{-q \pm \sqrt{q^2-4}}{2} \tag{3.17}$$

Combining this with the invariant-unity eigenvalue pair yields the six eigenvalues of the monodromy matrix in the CR3BP, the eigenvectors for which can be computed through use of $M\boldsymbol{v}_i^2 = \lambda_i \boldsymbol{v}_i$. If they exist, the stable and unstable eigenvalues are given by the smallest and largest real eigenvalues, respectively.

Differential Correction

Single-shooting

Construction of a Periodic Orbit using Differential Correction

We wish to demonstrate the techniques outlined in the previous section by computing a periodic orbit around a Lagrangian point L_i, and use this result to introduce the concept of stable and unstable manifolds. Section **??** outlines the mathematical relations behind the construction of such an orbit, and Section **??** provides information on its' implementation in a numerical computation package.

Establishing the differential correction routines

As mentioned in Section 3.3.1, the construction of a full periodic orbit around one of the Lagrangian points requires first the generation of a smaller 'seed' orbit to power the differential correction routines. For small amplitudes of periodic orbits, the linear approximation for Lagrangian motion outlined in Section 2.4, Equations **??** holds well. For arbitrarily larger values of amplitude and energy, a nonlinear analytical approximation to motion about a point L_i is required. For this, the reader is directed to OPTIMAL TRAJECTORY DESIGN TO HALO ORBITS.

The differential corrector provides an initial condition to a tolerance ϵ within a desired final condition, for $\epsilon << 1$, by variation of some of the initial state conditions $\boldsymbol{x}_0 = [x_0, y_0, z_0, \dot{x}_0, \dot{y}_0, \dot{z}_0]^T$.

$$|\boldsymbol{x}(t) - \boldsymbol{x}(0)| < \epsilon \tag{3.18}$$

If we take some flow mapping $\phi(t, t_0\ ;\ \boldsymbol{x}_0)$ from time $t_0 \rightarrow t$ whose trajectory is governed by the equations given in 2.23, and is of the form $\dot{\boldsymbol{x}}_0 = f(\boldsymbol{x})$, and seed some initial guess for a trajectory $\boldsymbol{x}_0$ that yields a perturbed trajectory at $t + \delta t$, $\boldsymbol{x}_0 + \delta \boldsymbol{x}_0$, we may express the displacement as follows:

$$\delta \boldsymbol{x}(t + \delta t) = \phi(t + \delta t, t_0;\ \boldsymbol{x}_0 + \delta \boldsymbol{x}_0) - \phi(t, t_0;\ \boldsymbol{x}_0) \tag{3.19}$$

Expansion of this into a Taylor Series about $t = t_1$ will yield:

$$\delta \boldsymbol{x}(t_1 + \delta t_1) = \frac{\partial \phi(t_1, t_0;\ \boldsymbol{x}_0)}{\partial \boldsymbol{x}_0} \delta \boldsymbol{x}_0 + \frac{\partial \phi(t_1, t_0;\ \boldsymbol{x}_0)}{\partial t_1 \delta t_1} + \text{higher order terms} \tag{3.20}$$

$$= \frac{\partial \phi(t_1, t_0;\ \boldsymbol{x}_0)}{\partial \boldsymbol{x}_0} \delta \boldsymbol{x}_0 + \dot{\boldsymbol{x}}_1 \delta t_1 = \Phi(t_1, t_0) \delta \boldsymbol{x}_0 + \dot{\boldsymbol{x}}_1 \delta t_1 + \text{higher order terms} \tag{3.21}$$

and, assuming we have some desired end-state

$$\boldsymbol{x}(t_1) = \phi(t_1, t_0;\ \boldsymbol{x}_0) = \boldsymbol{x}(t_1) = \boldsymbol{x}_d - \delta \boldsymbol{x}_1 \tag{3.22}$$

which is perturbed such that our actual state $\boldsymbol{x}_1$ is perturbed from our desired state $\boldsymbol{x}_1$ by an amount $\delta \boldsymbol{x}_1$, $\delta \boldsymbol{x}_1 > \epsilon$, we may quantify the change in initial conditions to attempt convergence through revisiting the state transition matrix:

$$\phi(t_1, t_0;\ \boldsymbol{x}_0 + \delta \boldsymbol{x}_0) = \phi(t_1, t_0; \boldsymbol{x}_0) + \frac{\partial \phi(t_1, t_0;\ \boldsymbol{x}_0)}{\partial \boldsymbol{x}_0} \delta \boldsymbol{x}_0 + \text{higher order terms} \tag{3.23}$$

$$= \phi(t_1, t_0; \boldsymbol{x}_0) + \Phi(t_1, t_0) \delta \boldsymbol{x}_0 + \text{higher order terms} \tag{3.24}$$

$$= \boldsymbol{x}_1 + \delta \boldsymbol{x}_1 + \text{higher order terms} \tag{3.25}$$

$$= x_d + \text{higher order terms} \tag{3.26}$$

which implies a change in initial conditions $\boldsymbol{x}_0$ by $\delta\boldsymbol{x}_0 = \Phi(t, t_0)^{-1}\delta\boldsymbol{x}_1$. This change will continue until such a point that

$$| \phi(t_1, t_0;\ \boldsymbol{x}_0 + \Delta\boldsymbol{x}_0) - x_d | < d \tag{3.27}$$

Inserting some specifics to the application of this differential correction to the design of a periodic orbit about a Lagrangian point, for simplicity, we seek symmetrical solutions, ones where the transformation

$$y \to -y,\ t \to -t \tag{3.28}$$

leaves the governing Equations in 2.23 unchanged. As such, we require the computation of only one northern or southern 'half' of the periodic orbit. Choosing an initial condition that intersects the x-axis of the system at 90°, and restricting the motion to the planar case, such that z and $\dot{z}$ are 0:

$$\boldsymbol{x}_0 = [x_0, 0, 0, v_y]^T \tag{3.29}$$

we integrate this to a set of conditions (Section 3.4.2) to obtain $\boldsymbol{x}(t_1)$ at the x-axis crossing; from this, we can compute $\Phi(t_1, 0)$. We desire our state at time $t = t_1$ to be:

$$\boldsymbol{x}(T/2) = \left[x_1, 0, 0, v_{y_{T/2}}\right]^T \tag{3.30}$$

with T as the period of the orbit, and where v_x is sufficiently small to be approximated to be zero. We may adjust the initial conditions through use of $\delta\boldsymbol{x}_0 = \Phi(t, t_0)^{-1}\delta\boldsymbol{x}_1$, holding x_0 fixed whilst adjusting v_{x_1}, and calculating the v_{y_0} correction through the following:

$$\delta v_{x_1} = \Phi_{34}\delta v_{y_0} + \dot{v}_{x_1}\delta t_1 + \text{higher order terms} \tag{3.31}$$

$$0 = \delta y_1 = \Phi_{24}\delta v_{y_0} - v_{y_1}\delta_{t_1} + \text{higher order terms} \tag{3.32}$$

where Φ_{ij} is matrix element in column i and row j, and $\dot{v}_{x_1}$ comes from the equations of motion. Since $v_{x_1} = 0$, $\delta v_{x_1} = v_{x_1}$, and thus:

$$\delta v_{y_0} \approx \left(\Phi_{34} - \frac{v_{x_1}}{v_{y_1}}\Phi_{24}\right)^{-1} v_{x_1} \tag{3.33}$$

Implementation of the techniques for orbit construction

Figure 3.1 represents the software runtimes necessary to generate a periodic orbit in the three-body problem. For the remainder of this section, the syntax for the implementation of this computation will be MATLAB-specific, although the heuristics of the work is easily translated into any other computation languages, such as Fortran or Python.

We first begin by creating the model of the governing equations of motion for the three-body problem. For this case, we restrict the problem to planar motion. Using the governing equations defined in 2.23,and neglecting the out-of-plane terms, the following parameters are set:

$$x = \begin{bmatrix} x \\ y \\ \dot{x} \\ \dot{y} \end{bmatrix} \dot{x} = \begin{bmatrix} \dot{x} \\ \dot{y} \\ \dot{v}_x \\ \dot{v}_y \end{bmatrix} \tag{3.34}$$

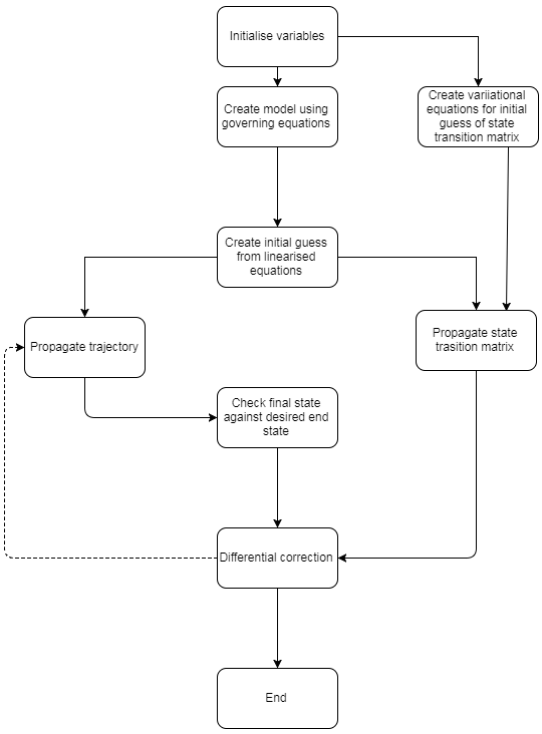

Figure 3.1: Software system architecture for the construction of a periodic orbit about a Lagrangian point.

with each initialised through use of a MATLAB vector array, and accessible through the respective array index. v_x and v_y are made available through the governing equations of motion, whilst all other terms are updated by the numerical integration routine.

We now go on to create the variational equations for use in the orbit creation; noting that we are limiting this case to a planar orbit, some modifications of the Jacobian matrix [‡] are required. Recalling equation 3.2, and neglecting the U_{xz}, U_{zx}, U_{yz}, U_{zy} terms, and reducing I_3 to I_2 whilst reducing Ω to be 2x2, yields:

$$A(t) = \begin{bmatrix} 0 & I_2 \\ U_{\text{restricted}} & 2\Omega_{\text{restricted}} \end{bmatrix} \tag{3.35}$$

which we may represent into a model in MATLAB by determining the three double-partial derivatives of the potential function $U(x, y)$ to be

$$U_{xx} = -1 + \frac{m_1}{r_{13}^{3/2}}\left(1 - \frac{3(x+m_2)^2}{r_{13}}\right) + \frac{m_2}{r_{23}^{3/2}}\left(1 - \frac{3(x-m_1)^2}{r_{23}}\right) \tag{3.36}$$

$$U_{yy} = -1 + \frac{m_1}{r_{13}^{3/2}}\left(1 - \frac{3y^2}{r_{13}}\right) + \frac{m_2}{r_{23}^{3/2}}\left(1 - \frac{3y^2}{4_{23}}\right) \tag{3.37}$$

$$U_{xy} = -\frac{m_1(3y(x+m_2))}{r_{13}^{5/2}} - \frac{m_2(3y(x-m_1))}{r_{13}^{5/2}} \tag{3.38}$$

[‡]Another term for $A(t)$

Moving on to creating the initial guess from the linearised equations, we refer to (Richardson, 1980). Taking the linearised equations of motion about the Lagrange points reference in Equation **??**:

$$\ddot{x} - 2\dot{y} - (1 + 2c_2)x = 0 \tag{3.39}$$

$$\ddot{y} + 2\dot{x} + (c_2 + 1)y = 0 \tag{3.40}$$

$$\ddot{z} + \lambda^2 z = 0 \tag{3.41}$$

we obtain a solution in terms of k, c_2 and λ, referenced in **??**. Using these as initial solutions, with λ as the center eigenvalue, yields:

$$x = \text{Earth-Sun } L_i \text{ distance} - A_x \tag{3.42}$$

where k is equal to:

$$\frac{1}{2\lambda}\left(\lambda^2 + 1 + 2c_2\right) \tag{3.43}$$

and c_2 is equal to:

$$c_2 = \frac{1}{\gamma^3}\left(\mu + \frac{(1-\mu)\gamma^3}{(1-\gamma)^3}\right) \tag{3.44}$$

with v_y equal to:

$$v_y = \frac{\mathrm{d}}{\mathrm{d}t}\left(kA_x \sin\lambda s + \psi\right) = kA_x\lambda \tag{3.45}$$

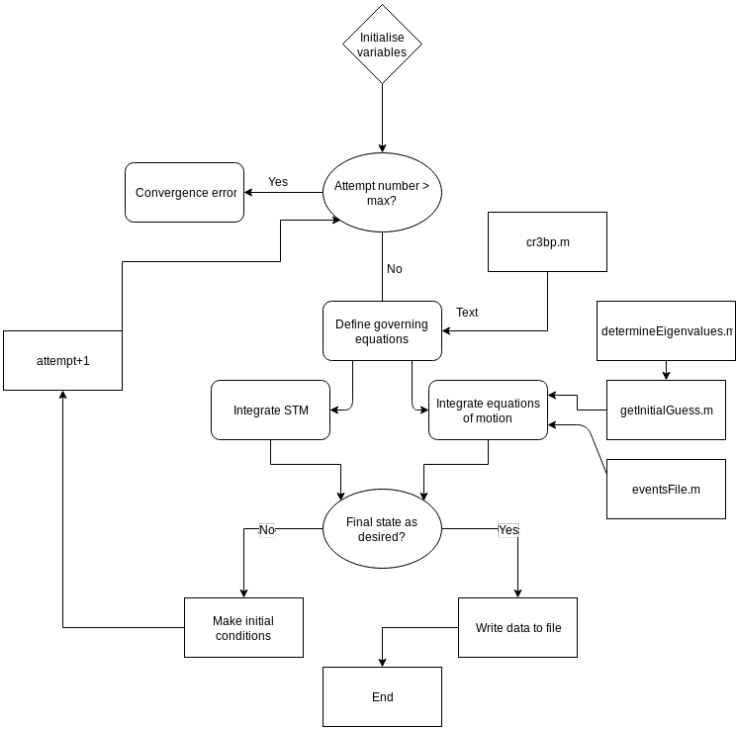

Figure 3.2: Differential correction software flow diagram

4

Introduction to Manifold Structures

References

Belbruno, E. (2004). *Capture Dynamics and Chaotic Motions in Celestial Mechanics*. Princeton University Press.

Belbruno, E. and Miller, J. (1993). Sun-perturbed Earth-to-moon transfers with ballistic capture. *Journal of Guidance Control and Dynamics 16*.

Broucke, R. A. (1968). *Periodic orbits in the restricted three-body problem with earth-moon masses*.

Curtis, H. D. (2010). *Orbital Mechanics for Engineering Students*. Elsevier, Oxford, 2nd edition.

Euler, L. (1736). *Mechanica sive motus scientia analytice exposita*.

Heath, T. L. and Euclid (1956). *The Thirteen Books of Euclid's Elements, Books 1 and 2*. Dover Publications, Incorporated.

Hill, G. (1906). *Collected Mathematical Works*.

Howell, K., Barden, B. T., and Wilson, R. S. (1997). Trajectory design using a dynamical systems approach with applications to GENESIS. In *AIAA Special Astrodynamics Conference*, page 33, Sun Valley, Idaho. AAS Publications Office.

Jacobi, C. G. J. (1829). Fundamenta Nova Theoriae Functionum Ellipticarum. *Regiomonti, Sumtibus fratrum Borntr\"ager*, page 189.

Mains, D. L. (1993). *Transfer trajectories from Earth parking orbits to L1 halo points.pdf*. PhD thesis, Purdue University.

Parker, J. S. and Anderson, R. L. (2014). Low-Energy Lunar Trajectory Design. *Low-Energy Lunar Trajectory Design*, (July):1–396.

Poincaré, H. (1899). *Les Méthodes Nouvelles de la Mécanique Céleste*. Gauthier-Villars.

Richardson, D. L. (1980). Halo Orbit Formulation for the ISEE-3 Mission. 3(6):543–548.

Russell, R. P. (2006). Global search for planar and three-dimensional periodic orbits near Europa. *The Journal of the Astronautical Sciences*, 54(2):199–226.

Szebehely, V. G. (1967). *Theory of Orbits - The Restricted Problem of Three Bodies*. Academic Press.

Vicens, J. R. (2016). *Regularization in Astrodynamics : applications to relative motion, low-thrust missions, and orbit propagation*. PhD thesis, Universidad Politecnica de Madrid.